ICA 2016 BUENOS AIRES
Buenos Aires – 5 to 9 September 2016
Acoustics for the 21st Century...

PROCEEDINGS of the 22nd International Congress on Acoustics

Numerical Computation in Musical Acoustics: Paper ICA2016-560

Modelling collisions of nonlinear strings against rigid barriers: Conservative finite difference schemes with application to sound synthesis

Michele Ducceschi[(a)], **Stefan Bilbao**[(b)], **Charlotte Desvages**[(c)]

[(a)]Acoustics and Audio Group, University of Edinburgh, UK, michele.ducceschi@ed.ac.uk
[(b)]Acoustics and Audio Group, University of Edinburgh, UK, sbilbao@staffmail.ed.ac.uk
[(c)]Acoustics and Audio Group, University of Edinburgh, UK, charlotte.desvages@ed.ac.uk

Abstract

Strings are common elements found in many musical instruments. Various models of string dynamics exist, describing cases of increasing complexity. For fine-grained simulation of string dynamics, either in the context of musical acoustics investigation or for sound synthesis, linear models such as the wave equation with stiffness are, however, insufficient. Recent work has focused on the coupling of a Kirchhoff-Carrier nonlinear string model with collisions against lumped or distributed barriers, showing promising results. The collisions are described by means of a penalty potential, relying on a fictitious interpenetration but allowing a description within an energy-balanced framework. In this work, the same collision model is used, but the nonlinear string model is further developed, in order to allow complex modal coupling rules, as well as amplitude-dependent pitch. In order to handle such complex system, appropriate finite difference schemes are developed, using energy-balanced methods. Results of simulations are presented, along with some applications to sound synthesis.

Keywords: nonlinear string vibrations, Finite Difference schemes, collisions, musical acoustics

Modelling collisions of nonlinear strings against rigid barriers: Conservative finite difference schemes with application to sound synthesis

1 Introduction

Nonlinear string vibration represents a fundamental problem in musical acoustics. Nonlinearities may appear as a consequence of large strains in the string, but also due to collisions against frets, fret boards and of course mallets, picks and fingers. Nonlinearities of geometric type have been studied in a number of works [1, 15, 5, 7]. On the other hand, a general energy-balanced framework for collisions of strings against lumped or distributed objects has recently been developed, showing promising results [4]. In this work, a geometrically nonlinear string model (with local nonlinearity) is coupled to a colliding object acting at the input, and the string is in distributed but intermittent contact with a rigid barrier.

Model equations are presented in Section 2; Finite difference schemes are developed in Section 3, and numerical experiments are presented in Section 4: the case of an open D double bass string is investigated in some detail.

2 Model Equations

In this work, nonlinear string vibration in a single polarisation is considered. The string is defined over a spatial domain $\mathscr{D} \triangleq [0, L_0]$. One possible model to describe such vibrations is the following system:

$$\rho A\, w_{,tt} = T_0\, w_{,xx} - EI \boxdot w_{,xxxx} + \frac{EA - T_0}{2} \left(w_{,x}^3 + 2 w_{,x} \zeta_{,x} \right)_{,x} - 2\sigma_0^{(t)} w_{,t} + 2\sigma_1^{(t)} w_{,txx} - \Upsilon \widehat{f} + \widetilde{f} \tag{1a}$$

$$\rho A\, \zeta_{,tt} = EA \zeta_{,xx} + \frac{EA - T_0}{2} \left(w_{,x}^2 \right)_{,x} - 2\sigma_0^{(l)} \zeta_{,t} + 2\sigma_1^{(l)} \zeta_{,txx} \tag{1b}$$

$$M\, W_{,tt} = \widehat{f} \tag{1c}$$

The various constants appearing in the model above are: volumetric density ρ, cross section A, string tension T_0, Young's modulus E, area moment of inertia I. $\sigma_0^{(t)}$, $\sigma_1^{(t)}$, $\sigma_0^{(l)}$, and $\sigma_1^{(l)}$ are non-negative constants allowing for the modeling of frequency-dependent loss (both transverse and longitudinal).

In the system, symbols after commas denote derivatives with respect to t and x. The two dependent variables are $w(x,t)$ and $\zeta(x,t)$. and represent, respectively, the transverse displacement and the longitudinal displacement. For a point on the string located at $(x,0)$ at rest; under displacement, the point will be located at $(x+\zeta, w)$.

A colliding object of mass M and transverse coordinate $W(t)$, acting as input excitation, is also included as per (1c). The symbol Υ in (1a) denotes a spreading distribution such that $\int_0^{L_0} \Upsilon \, \mathrm{d}x = 1$; this is the region on the string corresponding to the collision. (In the case of pointwise interaction at $x = x_f$, $\Upsilon \triangleq \delta(x - x_f)$.) The terms $\widehat{f}, \widetilde{f}$ are forcing terms, and will be considered in some detail below.

The operator $\boxdot$ in (1a) is defined as

$$\boxdot \triangleq \left(1 - \frac{EI}{A\kappa G} \frac{\partial^2}{\partial x^2} \right)^{-1} \tag{2}$$

From the definition, it is seen that the operator $\boxdot$ reduces to the identity operator at large wavelengths. In such a limit, the stiffness term of (1a) reduces to the well-known Euler-Bernoulli stiffness term,

used in many works for linear strings [9, 3, 10, 12] . More recent works [7, 8] have employed a Timoshenko-like stiffness term in order to overcome the problem of unbounded group velocity arising in the Euler-Bernoulli model. Here, a correction to the Euler-Bernoulli stiffness due to the *shear beam model* is considered, as per (2). This correction allows for bounded group velocity, giving asymptotic behaviour similar to that of the Timoshenko lower branch, despite the lack of explicit dependence on the shear angle [13, 14, 11].

The nonlinear term appears here as per the well-known model first used by Anand [1] and by Morse and Ingard [15] and later by other authors [5, 6, 2]. Such a model results from a series approximation to the geometrical nonlinearity in the string at large amplitudes. The approximated generating potential, despite not being geometrically exact, yields simplified equations which are more tractable from both analytical and numerical standpoints. A form for such potential will be given in 2.1, where an energy analysis of the system is performed.

The function $\widehat{f} = \widehat{f}(t)$ in (1a) is the force of interaction between the mass M and the string, with spatial distribution Υ. The function $\widetilde{f} = \widetilde{f}(x,t)$ in (1a) is the distributed force per unit length that the barrier exerts on the string. Following [4], one may express all such forces by means of a generating potential function, in the following way

$$\widehat{f} = \frac{\phi_{,t}(\widehat{\eta}, K_M, \alpha_M)}{\widehat{\eta}_{,t}}, \qquad \widetilde{f} = \frac{\phi_{,t}(\widetilde{\eta}, K_b, \alpha_b)}{\widetilde{\eta}_{,t}}. \tag{3a}$$

$$\widehat{\eta} = \langle w, \Upsilon \rangle_{\mathscr{D}} - W, \qquad \widetilde{\eta} = b - w. \tag{3b}$$

The variables denoted by $\widehat{\eta}, \widetilde{\eta}$ in (3b) can be thought of as a measure of the amount of interpenetration when two objects are colliding. K_M and K_b are the stiffness parameters of the colliding mass and of the barrier, respectively; α_M and α_b are characteristic exponents. The potential ϕ has the following form

$$\phi(x, K, \alpha) \triangleq \frac{K}{\alpha+1} [x]_+^{\alpha+1}, \quad \alpha \geqslant 1, \quad [x]_+ \triangleq \frac{1}{2}(x + |x|). \tag{4}$$

It is seen that the potential is nonzero if and only if its argument is positive, i.e. when the objects are in contact.

2.1 Energy, Boundary Conditions and Bounds on Solution Growth

An energy analysis is now performed for system (1). This allows the derivation of some bounds on the growth of the solution, as well as to derive suitable boundary conditions. For that, the L_2 inner product of two well-behaved functions $f(x), g(x)$ over $\mathscr{D}$ and related norm is indicated as

$$\langle f, g \rangle_{\mathscr{D}} \triangleq \int_0^{L_0} f\, g \, \mathrm{d}x, \; \rightarrow \|f\|_{\mathscr{D}}^2 \triangleq \langle f, f \rangle_{\mathscr{D}}. \tag{5}$$

Inner products of the form of (5) are taken in the following way: (1a) with $w_{,t}$ and (1b) with $\zeta_{,t}$; (1c) is multiplied on both sides by $W_{,t}$. The equations are then summed together and integration by parts is performed, in order to obtain the energy of the system. For the sake of conciseness, the steps are not presented here, and the result for the total energy $\mathfrak{H}$ is given as

$$\frac{d}{dt}\mathfrak{H} \triangleq \frac{d}{dt}\left(\mathfrak{K} + \mathfrak{U}_l + \mathfrak{U}_{nl} + \mathfrak{U}_\phi\right) = -Q + B\Big|_0^{L_0}. \tag{6}$$

In the formula, $\mathfrak{K}$ is the kinetic energy, $\mathfrak{U}_l$ is the linear potential energy due to tension and stiffness of the string, $\mathfrak{U}_{nl}$ is the nonlinear potential function of the Morse model, $\mathfrak{U}_\phi$ is the potential energy

resulting form the collisions. On the right-hand side, Q is the power loss due to dissipation, and B represents boundary terms. Remembering the definition of norm, explicit forms are given as

$$\mathfrak{K} = \frac{\rho A}{2}\|w_{,t}\|^2_{\mathscr{D}} + \frac{\rho A}{2}\|\zeta_{,t}\|^2_{\mathscr{D}} + \frac{M}{2}W_{,t}^2; \quad \mathfrak{U}_l = \frac{T_0}{2}\|w_{,x}\|^2_{\mathscr{D}} + \frac{T_0}{2}\|\zeta_{,x}\|^2_{\mathscr{D}} + \frac{A\kappa G}{2}\|w_{,x} - \vartheta\|^2_{\mathscr{D}} + \frac{EI}{2}\|\vartheta_{,x}\|^2_{\mathscr{D}}$$

$$\mathfrak{U}_{nl} = \frac{EA - T_0}{8}\|w_{,x}^2 + 2\zeta_{,x}^2\|_{\mathscr{D}}, \quad \mathfrak{U}_\phi = \phi(\widehat{\eta}) + \langle 1, \phi(\widetilde{\eta})\rangle_{\mathscr{D}}$$

$$Q = 2\sigma_0^{(t)}\|w_{,t}\|^2_{\mathscr{D}} + 2\sigma_1^{(t)}\|w_{,xt}\|^2_{\mathscr{D}} + 2\sigma_0^{(l)}\|\zeta_{,t}\|^2_{\mathscr{D}} + 2\sigma_1^{(l)}\|\zeta_{,xt}\|^2_{\mathscr{D}}$$

$$B = T_0 w_{,x} w_{,t} + A\kappa G(w_{,x} - \vartheta)w_{,t} + EI\vartheta_{,x}\vartheta_{,t} + EA\zeta_{,x}\zeta_{,t} + \frac{EA - T_0}{2}(w_{,x}^3 + 2w_{,x}\zeta_{,x}^3)w_{,t} + \frac{EA - T_0}{2}w_{,x}^2\zeta_{,t}.$$

where the shear angle is defined as

$$\vartheta = \boxdot w_{,x},$$

The total energy is positive semi-definite. Notice that, for vanishing B at the boundaries, and for $\sigma_0^{(t),(l)}, \sigma_1^{(t),(l)} \geqslant 0$, the system is non-strictly dissipative. In particular, when the boundary term vanishes, one can bound the growth of the solution in terms of the initial energy $\mathfrak{H}_0$, in the following way:

$$\|w_{,t}\|_{\mathscr{D}} \leqslant \left(\frac{2\mathfrak{H}_0}{\rho A}\right)^{1/2}. \tag{7}$$

Also, a bound on the amount of spurious interpenetration between the string and the barrier can be made as small as desired in the limit of $K_b \to \infty$ [4].

3 Finite Difference Schemes

Solutions to system (1) are now sought by means of appropriate finite difference schemes. Before doing so, some notation is introduced.

3.1 Discrete Inner Product and Norm

In a discrete setting, the domain of the problem ($\mathbb{D}$) is made up of M equally spaced points such that

$$\mathbb{D} = \{l, M \in \mathbb{Z}, 0 \leqslant l \leqslant M, L_0/M = h\}.$$

The parameter h is called the *grid spacing*. Time is discretised by means of a sampling rate $f_s = 1/k$, where k is the *time-step*. The dependent variables are now represented by grid functions, and unless otherwise specified they are evaluated at locations lh and at times nk, for $l \in \mathbb{D}_l$, $n \in \mathbb{Z}^+$. The definitions of inner product and norm for grid functions are

$$\langle f, g\rangle_{\mathbb{D}_l} \triangleq h\sum_{l=0}^{M} f_l g_l \quad \to \|f\|^2_{\mathbb{D}} \triangleq \langle f, f\rangle_{\mathbb{D}_l}. \tag{8}$$

Inner products on a different domain, lacking the left end point and denoted $\underline{\mathbb{D}}_l$, will also be used. Hence

$$\langle f, g\rangle_{\underline{\mathbb{D}}} \triangleq h\sum_{l=1}^{M} f_l g_l \quad \to \|f\|^2_{\underline{\mathbb{D}}} \triangleq \langle f, f\rangle_{\underline{\mathbb{D}}}.$$

3.2 Difference Operators

Finite difference operators are now defined. Identity, time-shifting and time difference operators are defined, with respect to a grid function w_l^n, as

$$1w^n = w^n; \quad e_{t+}w^n = w^{n+1}; \quad e_{t-}w^n = w^{n-1}, \quad \delta_{t+} \triangleq \frac{e_{t+}-1}{k}; \quad \delta_{t-} \triangleq \frac{1-e_{t-}}{k}; \quad \delta_{t\cdot} \triangleq \frac{e_{t+}-e_{t-}}{2k}, \quad \delta_{tt} \triangleq \delta_{t+}\delta_{t-}.$$

Time-averaging operators are defined as

$$\mu_{t+}\mu_{t-} \triangleq \frac{1+e_{t+}}{2}; \quad \mu_{t-} \triangleq \frac{1+e_{t-}}{2}; \quad \mu_{t\cdot} \triangleq \frac{e_{t+}+e_{t-}}{2}, \quad \mu_{tt} \triangleq \mu_{t+}\mu_{t-}.$$

Spatial difference operators are defined using an analogous notation. Hence, identity, space-shifting operators and space difference operators are defined,, agan for a grid function w_l^n, as

$$1w_l = w_l; \quad e_{x+}w_l = w_{l+1}; \quad e_{x-}w_l = w_{l-1}, \quad \delta_{x+} \triangleq \frac{e_{x+}-1}{h}; \quad \delta_{x-} \triangleq \frac{1-e_{x-}}{h}; \quad \delta_{x\cdot} \triangleq \frac{e_{x+}-e_{x-}}{2h}.$$

Second-order approximations to the second and fourth space derivatives are denoted as

$$\delta_{xx} \triangleq \delta_{x+}\delta_{x-} \quad \delta_{xxxx} \triangleq \delta_{xx}\delta_{xx}$$

3.3 Implementation

Finite Difference scheme for system (1) may be constructed in the following way

$$\rho A\delta_{tt}w = T_0\delta_{xx}w - EI\boxdot\delta_{xxxx}w + \frac{EA-T_0}{2}\mathfrak{N}^{(t)} - 2\sigma_0^{(t)}\delta_{t\cdot}w + 2\sigma_1^{(t)}\delta_{t\cdot}\delta_{xx}w - \Upsilon\widehat{f} + \widetilde{f} \tag{9a}$$

$$\mathfrak{N}^{(t)} = \delta_{x+}\left[(\delta_{x-}w)^2\mu_{t\cdot}(\delta_{x-}w) + 2(\delta_{x-}w)\mu_{tt}(\delta_{x-}\zeta))\right] \tag{9b}$$

$$\rho A\,\delta_{tt}\zeta = EA\delta_{xx}\zeta + \frac{EA-T_0}{2}\mathfrak{N}^{(l)} - 2\sigma_0^{(l)}\delta_{t\cdot}\zeta + 2\sigma_1^{(l)}\delta_{t\cdot}\delta_{xx}\zeta \tag{9c}$$

$$\mathfrak{N}^{(l)} = \delta_{x+}\left[(\delta_{x-}w)\mu_{t\cdot}(\delta_{x-}w)\right] \tag{9d}$$

$$M\delta_{tt}W = \widehat{f} \tag{9e}$$

In analogy with the continuous case, the shear correction operator is here defined as

$$\boxdot \triangleq \left(1 - \frac{EI}{A\kappa G}\delta_{xx}\right)^{-1} \tag{10}$$

The forcing term are expressed as

$$\widehat{f} = \frac{\delta_{t\cdot}\phi(\widehat{\eta}, K_M, \alpha_M)}{\delta_{t\cdot}\widehat{\eta}}, \qquad \widetilde{f} = \frac{\delta_{t\cdot}\phi(\widetilde{\eta}, K_b, \alpha_b)}{\delta_{t\cdot}\widetilde{\eta}}. \tag{11a}$$

$$\widehat{\eta} = \langle w, \Upsilon\rangle_{\mathbb{D}_l} - W, \qquad \widetilde{\eta} = b - w. \tag{11b}$$

3.4 Discrete Energy, Boundary Conditions and Bounds on Solution Growth

A discrete quantity related to the energy of the system is conserved. To show this, one can take discrete inner products of the form (8): (9a) and (9c) with, respectively, $\delta_{t\cdot}u$ and $\delta_{t\cdot}\zeta$; (9e) is multiplied on both sides by $\delta_{t\cdot}W$. The equations are then summed and summation by parts is employed. The

steps are lengthy and some care must be taken when handling the operator $\boxdot$. For the sake of conciseness, they are not reported here. The result is given as

$$\delta_{t+}\mathfrak{h} \triangleq \delta_{t+}\left(\mathfrak{k}+\mathfrak{u}_l+\mathfrak{u}_{nl}+\mathfrak{u}_\phi\right) = -\mathfrak{q}+\beta_{\rightarrow}-\beta_{\leftarrow}. \tag{12}$$

In the formula, $\mathfrak{k}$ are the kinetic terms, $\mathfrak{u}_l$ are the linear potential terms coming from tension and stiffness, $\mathfrak{u}_{nl}$ are the nonlinear potential terms and $\mathfrak{u}_\phi$ is the energy stored in the collisions. On the right hand side, q is a term representing power losses due to dissipation, and $\beta_{\leftarrow}$, $\beta_{\rightarrow}$ are the boundary terms at, respectively, the left and the right end points. Explicitly

$$\mathfrak{k} = \frac{\rho A}{2}\|\delta_{t-}w\|^2_{\mathbb{D}} + \frac{\rho A}{2}\|\delta_{t-}\zeta\|^2_{\mathbb{D}} + \frac{M}{2}(\delta_{t-}W)^2, \quad \mathfrak{u}_l = \frac{T_0}{2}\langle\delta_{x-}w, e_{t-}\delta_{x-}w\rangle_{\underline{\mathbb{D}}} + \frac{T_0}{2}\|\mu_{t-}\delta_{x-}\zeta\|^2_{\underline{\mathbb{D}}} - \frac{EAk^2}{8}\|\delta_{t-}\delta_{x-}\zeta\|^2_{\underline{\mathbb{D}}}$$
$$+ \frac{A\kappa G}{2}\langle\delta_{x-}w-\vartheta, e_{t-}(\delta_{x-}w-\vartheta)\rangle_{\underline{\mathbb{D}}} + \frac{EI}{2}\langle\delta_{x-}\vartheta, e_{t-}\delta_{x-}\vartheta\rangle_{\underline{\mathbb{D}}}$$

$$\mathfrak{u}_{nl} = \frac{EA-T_0}{8}\|2\mu_{t-}(\delta_{x-}\zeta) + (\delta_{x-}w)\,e_{t-}(\delta_{x-}w)\|^2_{\underline{\mathbb{D}}}, \quad \mathfrak{u}_\phi = \mu_{t-}\phi(\widehat{\eta}) + \langle 1, \mu_{t-}\phi(\widetilde{\eta})\rangle_{\mathbb{D}}$$

$$\mathfrak{q} = 2\sigma_0^{(t)}\|\delta_{t\cdot}w\|^2_{\mathbb{D}} + 2\sigma_1^{(t)}\|\delta_{t\cdot}\delta_{x-}w\|^2_{\underline{\mathbb{D}}} + 2\sigma_0^{(l)}\|\delta_{t\cdot}\zeta\|^2_{\mathbb{D}} + 2\sigma_1^{(l)}\|\delta_{t\cdot}\delta_{x-}\zeta\|^2_{\underline{\mathbb{D}}}$$

$$\beta_{\leftarrow} = EI(\delta_{t\cdot}\phi_0)(\delta_{x-}\phi_0) + (\delta_{t\cdot}w_0)((A\kappa G+T_0)\delta_{x-}w_0-\phi_{-1}) + EA(\delta_{t\cdot}\zeta_0)(\delta_{x-}\zeta_0)$$
$$+ \frac{EA-T_0}{2}\left[(\delta_{x-}w)^2\mu_{t\cdot}(\delta_{x-}w) + 2(\delta_{x-}w)\mu_{tt}(\delta_{x-}\zeta)\right]_1(\delta_{t\cdot}w_0) + \frac{EA-T_0}{2}\left[(\delta_{x-}w)\mu_{t\cdot}(\delta_{x-}w)\right]_1(\delta_{t\cdot}\zeta_0)$$

$$\beta_{\rightarrow} = EI(\delta_{t\cdot}\phi_{M-1})(\delta_{x+}\phi_{M-1}) + (\delta_{t\cdot}w_M)((A\kappa G+T_0)\delta_{x+}w_M-\phi_M) + EA(\delta_{t\cdot}\zeta_M)(\delta_{x+}\zeta_M)$$
$$+ \frac{EA-T_0}{2}\left[(\delta_{x-}w)^2\mu_{t\cdot}(\delta_{x-}w) + 2(\delta_{x-}w)\mu_{tt}(\delta_{x-}\zeta)\right]_{M+1}(\delta_{t\cdot}w_M) + \frac{EA-T_0}{2}\left[(\delta_{x-}w)\mu_{t\cdot}(\delta_{x-}w)\right]_{M+1}(\delta_{t\cdot}\zeta_M)$$

where the shear angle is

$$\vartheta = \delta_{x-}\boxdot w.$$

It is seen that the power loss q is strictly negative for $\sigma_0^{(t),(l)} > 0$, $\sigma_1^{(t),(l)} > 0$. Also, $\mathfrak{u}_\phi$ is positive definite, by definition of ϕ.

In the lossless case, and assuming that the boundary terms vanish, one may go further and bound the total energy from below. This is a rather lengthy proof and it is not shown here. The bound is

$$2h^2\mathfrak{h} \geqslant \left(h^2-h^2_{(t)}\right)\|\delta_{t-}w\|^2_{\underline{\mathbb{D}}} + \left(h^2-h^2_{(l)}\right)\|\delta_{t-}\zeta\|^2_{\underline{\mathbb{D}}}, \tag{13}$$

where

$$h^2_{(t)} = \frac{T_0k^2 - 4\frac{\rho EI}{\kappa G} + \left[\left(T_0k^2-4\frac{\rho EI}{\kappa G}\right)^2 + 16\rho AEIk^2\left(1+\frac{T_0}{A\kappa G}\right)\right]^{1/2}}{2\rho A}, \tag{14a}$$

$$h^2_{(l)} = \frac{E}{\rho}k^2. \tag{14b}$$

Hence, the energy is non-negative if $h^2 \geqslant \max[h^2_{(t)}, h^2_{(l)}]$. Assuming such inequality to be enforced, one may derive a bound analogous to (7). Hence, given an initial energy $\mathfrak{h}_0$, one has

$$\|\delta_{t-}w\|_{\mathbb{D}} \leqslant \left(\frac{2\mathfrak{h}_0}{\rho A}\right)^{1/2}. \tag{15}$$

3.5 Interpolation

For musical strings, $h_{(l)}^2$ is much larger than $h_{(t)}^2$, by typically a factor of ten. This reflects the fact that the longitudinal waves are faster than the transverse waves. Hence, for a given sampling rate, the choice $h^2 = h_{(l)}^2$ would result in a severe bandwith loss for the transverse wave field. This problem can be circumvented by oversampling, see for example [2]. A practical alternative, both cheaper and with improved numerical dispersion, is represented by interpolation. In practice, one chooses two work with two grid sizes, each one defined by the transverse and longitudinal space steps (14a), (14b), and interpolates between the grids [6]. This can be accomplished considering a modification of (9b) and (9d), in the following way

$$\mathfrak{N}^{(t)} = \delta_{x+}^{(t)} \left[(\delta_{x-}^{(t)} w)^2 \mu_{t\cdot} (\delta_{x-}^{(t)} w) + 2 (\delta_{x-}^{(t)} w) \mu_{tt} (\delta_{x-}^{(t)} \mathscr{I}_U \zeta)) \right], \qquad \mathfrak{N}^{(l)} = \delta_{x+}^{(l)} \mathscr{I}_D \left[(\delta_{x-}^{(t)} w) \mu_{t\cdot} (\delta_{x-}^{(t)} w) \right],$$

where $\mathscr{I}_U$, $\mathscr{I}_D$ are the upsampling and downsampling operators, related by the transpose operator:

$$\mathscr{I}_U = \frac{h_{(t)}}{h_{(l)}} \left(\mathscr{I}_D{}^T \right).$$

3.6 Numerical Dispersion

Because of numerical dispersion, scheme (9a) severely underestimates the eigenfrequencies in the middle and high ranges, and as a result the simulations sound flat. Again, one could circumvent this problem by oversampling, but a better strategy is to make use of one or more free parameters that can be adjusted to obtain better accuracy. For the case under study, a particularly attractive choice is represented by considering the following modifications to the opertators appearing in (9a):

$$\delta_{tt} \to \delta_{tt} \left[1 - \frac{\varepsilon_1}{4} k^2 \delta_{tt} \right]^{-1}, \qquad \boxdot \to \left[1 - \frac{EI}{A\kappa G} \delta_{xx}^{(t)} - \frac{\varepsilon_2}{4} h_{(t)}^2 \delta_{xx}^{(t)} \right]^{-1}$$

where the free parameters have been denoted by ε_1, ε_2 (notice that consistency is preserved in the limit of $h_{(t)} \to 0$, $k \to 0$.) Best values can be estimated by applying an optimisation algorithm in order to minimise dispersion (gradient descent was used here.) For the case under study, at $k = 1/44100$

$$\varepsilon_1 = -0.3997, \quad \varepsilon_2 = -0.7682,$$

produce the dashed curves shown in Figure 1, a much better match than the original scheme. Notice as well that the space step $h_{(t)}$ must be modified accordingly. Given

$$A_h = \rho A (1 + \varepsilon_2), \quad B_h = -T_0 k^2 (1 + \varepsilon_1 + \varepsilon_2 + \varepsilon_1 \varepsilon_2) + 4 \frac{\rho E I \rho}{\kappa G}, \quad C_h = -4 E I k^2 \left(1 + \frac{T_0}{A \kappa G} \right) (1 + \varepsilon_1),$$

one has

$$h_{(t)}^2 (\varepsilon_1, \varepsilon_2) = \frac{-B_h + \sqrt{B_h^2 - 4 A_h C_h}}{2 A_h}, \tag{16}$$

which reduces to (14a) when $\varepsilon_1 = \varepsilon_2 = 0$.

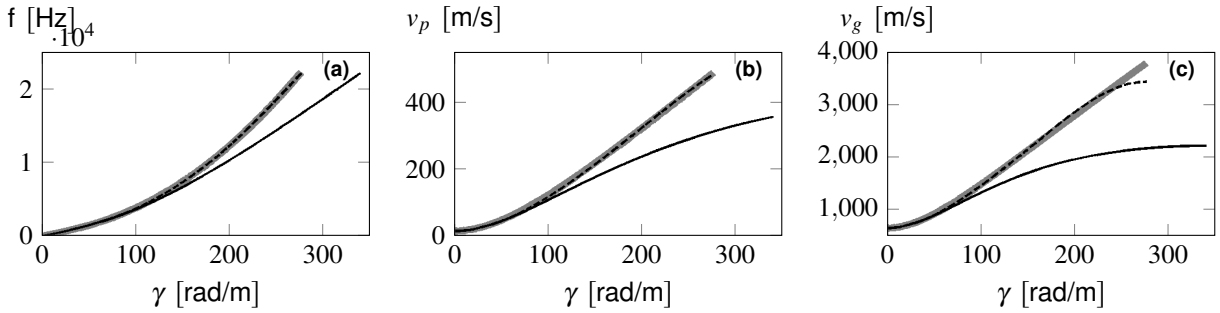

Figure 1: Linear dispersion relations for continuous model (thick grey line), scheme without free parameters (solid black line), optimised scheme (dashed black line). Reference string parameters given in section 4, time-step $k = 1/44100$. (a): frequency vs wavenumber; (b): phase velocity vs wavenumber; (c): group velocity vs wavenumber.

3.7 Matrix-Vector Update

Scheme (9) (and its improved versions making use of interpolation and free parameters) can always be cast in a convenient matrix-vector form, in the following way

$$\mathbf{Y}_{+1}^n \begin{bmatrix} w^{n+1} \\ \zeta^{n+1} \end{bmatrix} = \mathbf{Y}_0^n \begin{bmatrix} w^n \\ \zeta^n \end{bmatrix} + \mathbf{Y}_{-1}^n \begin{bmatrix} w^{n-1} \\ \zeta^{n-1} \end{bmatrix} + \begin{bmatrix} -\Upsilon \\ 0 \end{bmatrix} \widehat{f}^n + \begin{bmatrix} \widetilde{f}^n \\ 0 \end{bmatrix}, \tag{17a}$$

$$W^{n+1} = 2W^2 - W^{n-1} + \frac{k^2}{M} \widehat{f}. \tag{17b}$$

The matrices $\mathbf{Y}_{+1}^n$, $\mathbf{Y}_0^n$, $\mathbf{Y}_{-1}^n$ are square, sparse and time-dependent. Also, w, ζ, Υ and $\widetilde{f}$ are vectors, although they have not been printed in boldface type.

Because the forces are here defined in an implicit way, extra equations are needed in order to calculate their values are the timestep n. Suppose the matrix $\mathbf{Y}_{+1}^n$ is inverted in some manner (either explicitly or using a linear system solver); following [4] one can write a system of nonlinear equations to be solved for $\widehat{r}$, $\widetilde{r}$:

$$\widehat{r} - \widehat{\chi} + P \frac{\phi(\widehat{r} + \widehat{\eta}^{n-1}) - \phi(\widehat{\eta}^{n-1})}{\widehat{r}} - \left\langle \Upsilon, \mathbf{S} \frac{\phi(\widetilde{r} + \widetilde{\eta}^{n-1}) - \phi(\widetilde{\eta}^{n-1})}{\widetilde{r}} \right\rangle_{\mathbb{D}} = 0, \tag{18a}$$

$$\widetilde{r} - \widetilde{\chi} + \Upsilon \frac{\phi(\widehat{r} + \widehat{\eta}^{n-1}) - \phi(\widehat{\eta}^{n-1})}{\widehat{r}} + \mathbf{S} \frac{\phi(\widetilde{r} + \widetilde{\eta}^{n-1}) - \phi(\widetilde{\eta}^{n-1})}{\widetilde{r}} = 0. \tag{18b}$$

Consider the following known quantities

$$\tau_0 \triangleq \left(\left(\mathbf{Y}_{+1}^n\right)^{-1} \mathbf{Y}_0^n \begin{bmatrix} w^n \\ \zeta^n \end{bmatrix} \right)_{(0:N^{(t)})}, \quad \tau_{-1} \triangleq \left(\left(\mathbf{Y}_{+1}^n\right)^{-1} \mathbf{Y}_{-1}^n \begin{bmatrix} w^{n-1} \\ \zeta^{n-1} \end{bmatrix} \right)_{(0:N^{(t)})}$$

$$p \triangleq \left(\left(\mathbf{Y}_{+1}^n\right)^{-1} \begin{bmatrix} \Upsilon \\ 0 \end{bmatrix} \right)_{(0:N^{(t)})}, \qquad \mathbf{S} \triangleq \left(\left(\mathbf{Y}_{+1}^n\right)^{-1} \right)_{(0:N^{(t)}),(0:N^{(t)})},$$

where the subscript $(0:N^{(t)})$ denotes the first $N^{(t)}+1$ entries, for $N^{(t)} \triangleq L_0/h_{(t)}$. The constants appearing in (18) are then defined as

$$\widehat{\chi} = \langle \Upsilon, \tau_0 \rangle_{\mathbb{D}} + \langle \Upsilon, \tau_{-1} \rangle_{\mathbb{D}} - 2W^n + W^{n-1} - \hat{\eta}^{n-1}, \quad \widetilde{\chi} = w^{n-1} - \tau_0 - \tau_{-1}, \quad P = \langle p, \Upsilon \rangle_{\mathbb{D}} + \frac{k^2}{M}.$$

Once the nonlinear system (18) is solved for $\widehat{r}$, $\widetilde{r}$, one may use such quantities to calculate $\widehat{f}$, $\widetilde{f}$, using

$$\widehat{f} = \frac{\phi(\widehat{r} + \widehat{\eta}^{n-1}) - \phi(\widehat{\eta}^{n-1})}{\widehat{r}}, \quad \widetilde{f} = \frac{\phi(\widetilde{r} + \widetilde{\eta}^{n-1}) - \phi(\widetilde{\eta}^{n-1})}{\widetilde{r}}.$$

(Notice that the division in the expression for $\widetilde{f}$ is an element by element division, with a little abuse of notation.) Finally, such values are inserted in (17), which can be computed by means of a linear system solver.

4 Numerical Experiments

In order to illustrate the importance of the nonlinearities that come into play in musical string dynamics, the case for a double bass open D string is investigated. Simply-suppoted boundary conditions are chosen in the transverse direction ($w = \delta_{xx} w = 0$), and fixed conditions are chosen for the longitudinal waves ($\zeta = 0$). Table 1 reports the parameters for the string. Notice that the area A and moment of inertia I are calculated from the radius as

$$A = \pi r^2, \qquad I = \frac{\pi}{4} r^4.$$

The barrier, reported in the caption of Table 1, is tilted and runs up to 2/3 of the total string length. Figure 2 reports four different scenarios, of increasing nonlinearity. The strings are struck at high

	r (mm)	L_0	T_0	ρ	E (GPa)	κ	G (GPa)	$\sigma_0^{(t)}$	$\sigma_1^{(t)}$	$\sigma_0^{(l)}$	$\sigma_1^{(l)}$
$D2$	0.694	1.10	310	7860	200	0.89	77.7	$1.5{\cdot}10^{-3}$	$8{\cdot}10^{-5}$	$8{\cdot}10^{-2}$	$3{\cdot}10^{-6}$

Table 1: Case study: double-bass string $D2$. All units in SI, except where otherwise indicated. The barrier is $b(x) = -\tan\theta\, x$, for $\theta = \frac{\pi}{288}$ and $x \in [0, \frac{2}{3}L_0]$

.

amplitudes using the parameters in the caption of Figure 2. The waveforms cover the first three cycles of the string. It is interesting to notice how the geometrically nonlinear strings present a lower amplitude of vibration: this is expected as some energy is spent to activate the longitudinal modes. Perceptually, case (a) is the least interesting and case (d) is the richest: simulating a full "slap" gesture requires both the barrier *and* a geometrically nonlinear string; cases (b) and (c) are incomplete for this purpose. Nonetheless, it is useful to point out that the barrier plays a major role in the perceived sound quality, and perhaps it affects the output to a larger extent than the geometrical nonlinearity: this can be inferred by comparing the output spectra (b2) and (c2).

5 Conclusions

This work presented a nonlinear stiff string colliding against a distributed barrier and activated by a colliding object. Conservative Finite Difference schemes were presented in some detail, as well as numerical experiments to highlight the importance to include all nonlinearities to simulate typical string phenomena, such as a slapping gesture on the bass.

Acknowledgements

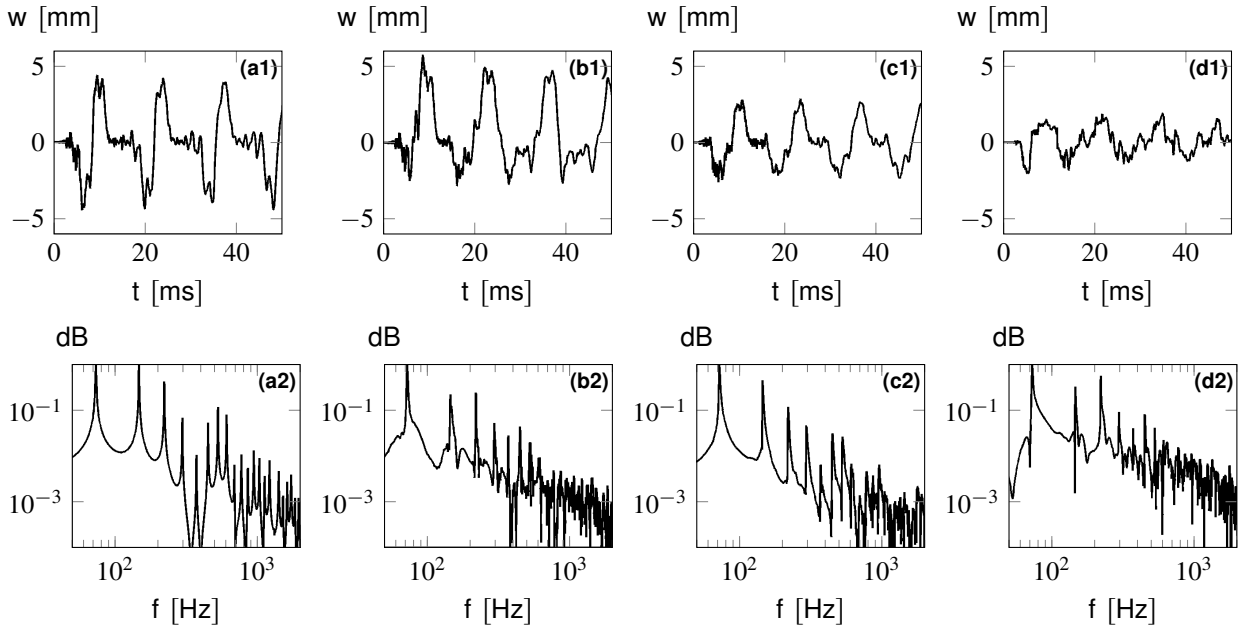

Figure 2: Trasverse displacements w and related spectra for: (a): linear string, no barrier; (b): linear string with barrier; (c): nonlinear string, no barrier; (d): nonlinear string with barrier. For all cases, output is taken at $0.22L_0$. The string is activated with a colliding object of mass M=10g, velocity 1m/s, α_M=1.3, $K_M = 5 \cdot 10^8$ hitting at $0.82L_0$.

This work was supported by the Royal Society and the British Academy, through a Newton International Fellowship, by the Edinburgh College of Art and the Audio Engineering Society Educational Foundation and by the European Research Council, under grant ERC-2011-StG-279068-NESS.

References

[1] G. Anand. Large-amplitude damped free vibration of a stretched string. *J. Acoust. Soc. Am.*, 45(5):1089–1096, 1969.

[2] B. Bank and L. Sujbert. Generation of longitudinal vibrations in piano strings: from physics to sound synthesis. *J. Acoust. Soc Am.*, 117(4):2268–2278, 2005.

[3] J. Bensa, S. Bilbao, R. Kronland-Martinet, and J. O. Smith. The simulation of piano string vibration: From physical models to finite difference schemes and digital waveguides. *J. Acoust. Soc. Am.*, 114(2):1095–1107, 2003.

[4] S. Bilbao, A. Torin and V. Chatziioannou. Numerical Modeling of Collisions in Musical Instruments. *Acta Acust. united Ac.*, 101(1):155–173, 2015.

[5] S. Bilbao. Conservative numerical methods for nonlinear strings. *J. Acoust. Soc. Am.*, 118(5):3316–3327, 2005.

[6] S. Bilbao. *Numerical Sound synthesis: Finite Difference Schemes and Simulation in Musical Acoustics*. Wiley, Chichester UK, 2009.

[7] J. Chabassier, A. Chaigne, and P. Joly. Modeling and simulation of a grand piano. *J. Acoust. Soc. Am.*, 134(1):648–665, 2013.

[8] J. Chabassier and S. Imperiale. Stability and dispersion analysis of improved time discretisation for prestressed Timoshenko systems. Application to the stiff piano string. *Wave Motion*, 50:456–480, 2013.

[9] A. Chaigne and A. Askenfelt. Numerical simulations of piano strings 1. A physical model for a struck string using finite difference methods. *J. Acoust. Soc. Am.*, 95(2):1112–1118, 1994.

[10] É Ducasse. On waveguide modeling of stiff piano strings. *J. Acoust. Soc. Am.*, 118(3):1776–1781, 2005.

[11] M Ducceschi and S. Bilbao. Linear stiff string vibrations in musical acoustics: assessment and comparison of models. *J. Acoust. Soc. Am.*, under review, 2016.

[12] N. Giordano. Finite difference modeling of the piano. *J. Acoust. Soc. Am.*, 119(5):3291–3291, 2006.

[13] K. F. Graff. *Wave Motion in Elastic Solids*. Dover Publications, New York, 1991.

[14] S.M. Han, H. Benaroya, and T. Wei. Dynamics of transversely vibrating beams using four engineering theories. *J. Sound Vib.*, 225(3):935–988, 1999.

[15] P. Morse and U. Ingard. *Theoretical Acoustics*. Princeton University Press, Princeton, New Jersey, 1968.